

Contents lists available at ScienceDirect

Chemical Engineering Research and Design

journal homepage: www.elsevier.com/locate/cherd

IChemE



Adsorption equilibrium of carbon dioxide on ammonia-modified activated carbon

Mohammad Saleh Shafeeyan^{a,*}, Wan Mohd Ashri Wan Daud^a,
Ahmad Shamiri^{a,b,*}, Nasrin Aghamohammadi^c

^a Department of Chemical Engineering, Faculty of Engineering, University of Malaya, 50603 Kuala Lumpur, Malaysia

^b Chemical & Petroleum Engineering Department, Faculty of Engineering, Technology & Built Environment, UCSI University, 56000 Kuala Lumpur, Malaysia

^c Centre for Occupational and Environmental Health, Department of Social and Preventive Medicine, Faculty of Medicine, University of Malaya, 50603 Kuala Lumpur, Malaysia

ARTICLE INFO

Article history:

Received 3 October 2014

Received in revised form 11 July 2015

Accepted 19 July 2015

Available online 29 July 2015

Keywords:

CO₂ adsorption

Activated carbon

Ammonia modification

Adsorption isotherm

Toth equation

Isosteric enthalpy

ABSTRACT

The equilibrium adsorption isotherms of carbon dioxide on a commercial granular activated carbon (GAC) and an ammonia-modified GAC (OXA-GAC) were measured using a static volumetric method. CO₂ adsorption measurements were performed at three different temperatures (303, 318, and 333 K), and pressures up to 1 atm. The obtained equilibrium data were fitted to the Freundlich, Sips, and Toth isotherms using a semi-empirical approach to differentiate the contributions of physical and chemical adsorption to the total CO₂ uptake. The isotherm parameters were determined independently for each mechanism by non-linear regression. To evaluate the adequacy of the fit of the isotherm models, two different error functions (i.e., the average relative error and the nonlinear regression coefficient) were calculated. The Toth semi-empirical equilibrium model provided the best fit to the experimental data, with average relative errors of less than 3% observed at all temperatures. The isosteric heats of CO₂ adsorption onto the ammonia-modified adsorbent and onto the untreated adsorbent were determined using the Clausius–Clapeyron equation. The loading dependence of the isosteric enthalpy of CO₂ adsorption over the OXA-GAC reflected an energetic heterogeneity of the adsorbent surface. The initial isosteric heats of adsorption of 70.5 kJ mol⁻¹ and 25.5 kJ mol⁻¹ correspond to the adsorption of CO₂ on the modified and untreated adsorbents, respectively, and these values were in excellent agreement with the zero-coverage heats of adsorption obtained using the temperature-dependent parameters of the proposed model.

© 2015 The Institution of Chemical Engineers. Published by Elsevier B.V. All rights reserved.

1. Introduction

Global warming and related environmental damage associated with emissions of carbon dioxide (CO₂), the most significant greenhouse gas, have long been recognized to represent a potential serious threat to the future of the earth's environment (Bezerra et al., 2011; Jadhav et al., 2007). The primary source of anthropogenic CO₂ emissions is the

combustion of fossil fuels such as coal or natural gas for the production of electricity (Mulgundmath and Tezel, 2010; Shafeeyan et al., 2014). Because fossil fuels are likely to remain the predominant energy source all over the world, CO₂ emissions must be reduced to mitigate the unfettered release of this greenhouse gas into the atmosphere (Garcés et al., 2013; Siriwardane et al., 2001). As a result, various CO₂ separation techniques, such as liquid solvent absorption, membrane

* Corresponding authors at: Department of Chemical Engineering, Faculty of Engineering, University of Malaya, 50603 Kuala Lumpur, Malaysia. Tel.: +60 3 79675297; fax: +60 3 79675319.

E-mail addresses: ms.shafeeyan@gmail.com (M.S. Shafeeyan), a.shamiri@um.edu.my (A. Shamiri).
<http://dx.doi.org/10.1016/j.cherd.2015.07.018>

0263-8762/© 2015 The Institution of Chemical Engineers. Published by Elsevier B.V. All rights reserved.

separation, cryogenic separation, and adsorption processes including pressure/vacuum swing adsorption (PSA/VSA) and temperature swing adsorption (TSA), are currently under investigation (Gomes and Yee, 2002; Xu et al., 2002). Currently, adsorption with amine-based adsorbents is the preferred technology for the large-scale separation of CO₂ from the flue-gas streams of fossil-fuel-based power plants. However, this method suffers from several significant drawbacks that impede its implementation, including low efficiency, high energy consumption during the regeneration process, a high equipment corrosion rate, oxidative degradation of the amines, and flow problems caused by viscosity (Houshmand et al., 2013; Rinker et al., 2000; Veawab et al., 1999). The development of alternative, lower cost, energy-efficient CO₂ removal technologies is therefore important.

The separation and purification of gas mixtures by adsorption is a potential option because of its ease of operation, high adsorption capacity, minimal environmental impact, low cost, and efficient recovery of the solute compared to conventional adsorption with liquid solvents (Cavenati et al., 2004; Houshmand et al., 2012; Serna-Guerrero et al., 2010a). Particularly, pressure-swing adsorption (PSA) has a number of attractive characteristics, such as its applicability over a relatively wide range of temperature and pressure conditions, its low energy requirements, and its low capital investment costs (Delgado et al., 2006; Mutasim and Bowen, 1991). The last three decades have seen a tremendous growth in research into and commercial applications of CO₂ removal from various flue-gas mixtures by PSA processes (Siriwardane et al., 2001; Yong et al., 2002). The development of an easily regenerated and durable adsorbent with fast adsorption/desorption kinetics, a high selectivity and a high adsorption capacity will undoubtedly enhance the competitiveness of adsorptive separation for CO₂ capture in flue-gas applications (Lu et al., 2009; Su et al., 2010). Among all adsorbents, activated carbon offers several advantages as a CO₂ adsorbent: an inherent affinity for CO₂, an easy-to-design pore structure, insensitivity to moisture, ease of regeneration, stability over a large number of cycles, and an appealing low cost (Bezerra et al., 2011; Houshmand et al., 2011a; Sjostrom and Krutka, 2010).

The CO₂ adsorption performance of activated carbon is well known to be strongly influenced by modification of the surface chemical properties of the activated carbon (Arenillas et al., 2005; Plaza et al., 2009; Shafeeyan et al., 2010). Inspired by the current liquid-phase amine scrubbing technology, researchers have incorporated different basic nitrogen functional groups onto the carbon surface for CO₂ removal from gaseous mixtures at relatively high temperatures (Przepiórski et al., 2004; Shafeeyan et al., 2015; Zhang et al., 2010). This approach is expected to exploit the strong chemical interactions between CO₂ and the attached basic nitrogen functionalities on the surface, as well as the low energy requirements, to regenerate the solid adsorbent (Drage et al., 2007; Houshmand et al., 2011b; Knowles et al., 2006; Maroto-Valer et al., 2005; Plaza et al., 2007). Several authors have proposed modifying activated carbon with gaseous ammonia in the presence or absence of oxygen as a suitable technique to produce efficient CO₂ adsorbents that maintain high uptakes despite moderately high temperatures (Pevida et al., 2008b; Plaza et al., 2009, 2010). In particular, in a previous study (Shafeeyan et al., 2012), a commercial granular activated carbon adsorbent was modified through an oxidation–amination process in an effort to increase its surface basicity and consequently enhance its CO₂ adsorption capacity. Because the results of this previous study indicated

that the ammonia-modified adsorbent exhibited promising properties in terms of working capacity, desorption capability and performance stability, this adsorbent's behavior was modeled for subsequent interpretation and simulation.

For the design and simulation of separation processes, the study of the adsorption equilibria is essential in supplying the basic information required for developing and validating models that represent the nature of the adsorption processes (Cavenati et al., 2004; Grande and Rodrigues, 2004). Although reliable experimental equilibrium data for some adsorbates on carbon adsorbents are extensively available in the literature (An et al., 2009; Garcés et al., 2013), as far as we know, very few data have been reported for CO₂ adsorption over ammonia-modified activated carbons under the conditions used here. Furthermore, no studies have been conducted to analyze the CO₂ adsorption isotherms over such adsorbents to fit to a proper isotherm model. Therefore, in the present paper, the adsorption equilibria of carbon dioxide over the parent GAC and its ammonia-modified counterpart (OXA-GAC) at various operating conditions were obtained and used to fit to an appropriate semi-empirical isotherm model. In a future study, the findings of the present work will be applied to develop and verify a mathematical model for describing the adsorption behavior of CO₂ on the ammonia-modified activated carbon in a fixed-bed adsorber.

2. Experimental and computational methods

2.1. Adsorbent materials

Earlier, our group optimized the amination conditions of activated carbon adsorbents in an effort to maximize their CO₂ adsorption/desorption capacities (Shafeeyan et al., 2012). The optimal adsorbent (a pre-oxidized sample that was aminated at 425 °C for 2.12 h) exhibited promising adsorption/desorption performance during cyclical operations, making it suitable for practical applications. Therefore, in this work, the optimal adsorbent (referred to as OXA-GAC) was used as a starting material. Further details on the adsorbent preparation and modification can be found elsewhere (Shafeeyan et al., 2011, 2012). The commercial granular palm-shell-based activated carbon (referred to as GAC) evaluated in the present paper was obtained from Bravo Green Sdn Bhd (Malaysia). The CO₂, N₂, and NH₃ used in the experiments were of purity greater than 99.99% and were supplied by Air Products.

2.2. Characterization of the adsorbents

N₂ adsorption/desorption at –196 °C using a Micromeritics ASAP 2020 analyzer aided the textural characterization of the samples. Prior to measurements, the samples were degassed for 12 h under vacuum at 130 °C. The Brunauer–Emmett–Teller (BET) specific surface area was calculated using adsorption data in the relative pressure (P/P_0) range of 0.04 to 0.2 (Sing, 1998). The total pore volume (V_{total}) was calculated from the amount of adsorbed N₂ at $P/P_0=0.99$. The micropore volume (V_{micro}) of the studied samples was estimated using the Dubinin–Radushkevich (DR) equation (Rouquerol et al., 1999).

2.3. CO₂ adsorption measurements

CO₂ adsorption–desorption isotherms of the modified and untreated activated carbon samples were measured using

a Micromeritics ASAP 2020 instrument, which is a static volumetric apparatus. The equilibrium experiments were conducted at temperatures of 30, 45 and 60 °C and at pressures up to 1 atm, a typical operating range in adsorption units for CO₂ capture from power plants. The adsorption temperature was controlled by circulating water from a thermostatic bath (Jeio Tech, model: Lab Companion RW 0525G) with an uncertainty of ±0.1 K. Using the volumetric method with P–V–T measurements, we determined the total quantity of gas introduced into the adsorption system and the quantity that remained in the system after reaching adsorption equilibrium. Prior to the CO₂ adsorption measurements, known amounts of samples (e.g., 50–100 mg) were loaded into the sample tube and degassed by reducing the pressure to 10^{−5} mmHg at 473 K for 15 h to dehydrate and desorb any adsorbed gases. CO₂ was then purged into the sample cell, and the change in adsorption volume as a function of CO₂ partial pressure was recorded. The final adsorption amount at the terminal pressure and temperature was considered to be the adsorption equilibrium amount.

2.4. Adsorption isotherm equations

For each modified and untreated activated carbon adsorbent, three isotherms were measured at 30, 45, and 60 °C and at pressures up to 1 atm. To apply the adsorption equilibrium data to a specific gas-separation application, an accurate mathematical representation of the adsorption equilibrium is required (Esteves et al., 2008). The equilibrium adsorption isotherm may provide useful insight into the adsorbate–adsorbent interactions and the surface properties and affinities of the adsorbent (Foo and Hameed, 2010). For this purpose, three different pure-species isotherm models – the Freundlich, Sips, and Toth isotherm equations – were used to correlate experimental equilibrium results. These three isotherm models are frequently used for modeling gas-separation processes.

The Freundlich isotherm can be applied to non-ideal adsorption on heterogeneous surfaces for a multilayer adsorption with a non-uniform distribution of adsorption heat. It is represented as (LeVan et al., 1999):

$$q = K_F P^{1/m_F} \quad (1)$$

The Sips isotherm is a combination of the Freundlich and the Langmuir isotherm models for predicting the behavior of heterogeneous adsorption systems. At low surface coverages, it reduces to the Freundlich equation, whereas, at high adsorbate concentrations, it predicts a monolayer adsorption capacity that is typical of the Langmuir isotherm. The Sips equation is given by (LeVan et al., 1999):

$$q = \frac{q_m (K_S P)^{1/m_S}}{1 + (K_S P)^{1/m_S}} \quad (2)$$

The Toth isotherm is a Langmuir-based isotherm derived from potential theory and is commonly used to describe heterogeneous adsorption processes. It considers a quasi-Gaussian distribution of site affinities. The Toth isotherm is written as (LeVan et al., 1999):

$$q = \frac{q_m K_T P}{(1 + (K_T P)^{m_T})^{1/m_T}} \quad (3)$$

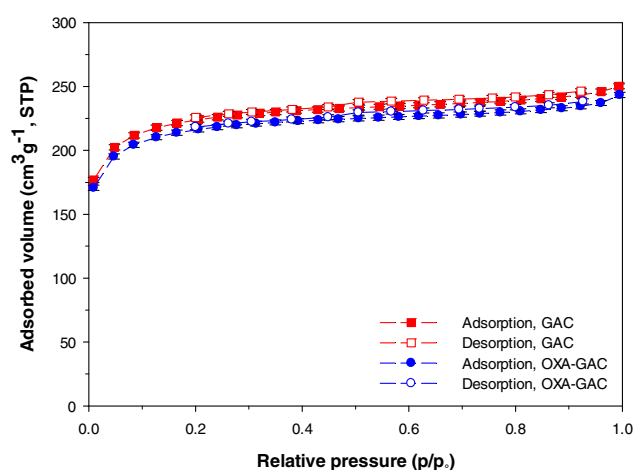


Fig. 1 – N₂ adsorption–desorption isotherms at –196 °C of the modified and untreated activated carbon adsorbents. The error bars represent the standard deviation based on triplicate analysis. For points where the error bars are not visible, the error bars are smaller than the symbols used.

In Eqs. (1)–(3), q represents the adsorbed concentration, P is the equilibrium pressure, q_m is the maximum loading capacity, K_i is the equilibrium constant (K_F) or the affinity parameter (K_S and K_T), and m_i (m_F , m_S , and m_T) is the parameter that refers to the system heterogeneity.

The next step is to fit the experimental equilibrium adsorption data to the aforementioned isotherm models and adjust each set of isotherm parameters. Because of the inherent bias associated with transforming non-linear isotherm equations into linear forms, several authors have proposed using a non-linear regression procedure (Ho et al., 2002; Porter et al., 1999). Accordingly, in the current study, the parameters of the isotherm equations for each temperature were obtained by non-linear regression analysis using the Marquardt–Levenberg algorithm implemented in SigmaPlot software version 12.0 (Systat Software Inc., USA), with a user-defined equation added to the Regression Wizard. To quantify and compare the goodness of fit of the above isotherm models to the experimental data and adjust each set of isotherm constants, two different error functions, the average relative error (ARE) and nonlinear regression coefficient (R^2), were evaluated. The average relative error, which measures the deviation between the experimental equilibrium data and the fitted model values, was calculated according to the following equation (Foo and Hameed, 2010):

$$\text{ARE}(\%) = \frac{100}{n} \sum_{i=1}^n \left| \frac{q_{\text{meas}} - q_{\text{cal}}}{q_{\text{meas}}} \right| \quad (4)$$

where n is the number of data points at a given temperature, and subscripts “meas” and “cal” refer to the measured and calculated values of q , respectively.

3. Results and discussion

3.1. Textural characterization

Fig. 1 represents the N₂ equilibrium adsorption isotherms at –196 °C for the untreated and the modified adsorbents. As evident in Fig. 1, the isotherms of both adsorbents are of the type I according to the BDDT (Brunauer, Deming, Deming and Teller)

Table 1 – Physical characteristics of the activated carbon adsorbents.

| Sample ID | S_{BET} ($\text{m}^2 \text{g}^{-1}$) | V_{total} ($\text{cm}^3 \text{g}^{-1}$) | V_{micro} ($\text{cm}^3 \text{g}^{-1}$) |
|-----------|---|--|--|
| GAC | 768 | 0.387 | 0.358 |
| OXA-GAC | 734 | 0.381 | 0.346 |

Classification (Do, 1998), indicating that the pore structure of the carbon samples is mainly composed of a well developed micropore volumes. Similarly, as evident from the figure, both adsorbents show hysteresis loops at $P/P_0 > 0.4$, which indicates the presence of certain mesoporosity in the samples. Table 1 lists the apparent surface area (S_{BET}), total pore (V_{total}) and micropore (V_{micro}) volumes of the activated carbon samples which are good measures to investigate relative changes in pore characteristics of these materials. The results showed that modification slightly decreases the apparent surface area, total pore and micropore volumes. For instance, the surface area of the modified adsorbent was of $734 \text{ m}^2 \text{ g}^{-1}$, which represents 95.6% of the surface area of the untreated adsorbent. The decrease in porous texture properties is probably due to the partially blockage of the micropore entrances by nitrogen functional groups that occurs during modification. However it can also be associated to the collapse of some adjacent pore walls during pre-oxidation stage leading to diminished micropore volumes (Rodríguez-Reinoso et al., 1991; Pereira et al., 2003)

3.2. Adsorption equilibrium study

The volumetric method of measuring adsorption involves measuring the pressure change in a known volume of gas introduced to an adsorbent sample. As the gas is adsorbed and allowed to reach equilibrium, the measured decrease in the closed-system pressure yields the amount of gas adsorbed under the given conditions (Li and Tezel, 2008). Adsorption and desorption isotherms of CO_2 obtained at temperatures of 30, 45 and 60°C and at pressures up to 1 atm for the ammonia-modified and untreated carbon are graphically represented in Fig. 2a and b, respectively. The ranges for temperature and pressure were chosen on the basis that a typical post-combustion flue gas contains approximately 10–15% CO_2 at a total pressure of 1 bar and a temperature range of 40– 60°C (Mason et al., 2011). As evident in these figures, for both modified and unmodified adsorbent, the concentration of adsorbed CO_2 increases with increasing pressure. At a given temperature, the shape of the function $M=f(P)$ (where M is the uptake at equilibrium pressure P) corresponded to a type I isotherm (i.e., a monotonically concave isotherm) according to the International Union of Pure and Applied Chemistry (IUPAC) classification scheme. A type I isotherm is typically characteristic of a microporous adsorbent.

The adsorption of CO_2 is well established to possibly result from physical and/or chemical factors both influencing the adsorbent performance (Drage et al., 2007; Maroto-Valer et al., 2005; Pevida et al., 2008a). For the unmodified adsorbent, CO_2 capture with a pure physisorption process was proposed as a controlling mechanism. As evident in Fig. 2a and b, in comparison with the unmodified adsorbent, OXA-GAC exhibited a higher CO_2 uptake, particularly at low partial pressures, as reflected by the steep initial slope of the isotherms. This enhanced uptake stems from adsorption by the nitrogen functional groups in addition to CO_2 capture by physical adsorption (Belmabkhout and Sayari, 2009). As the CO_2

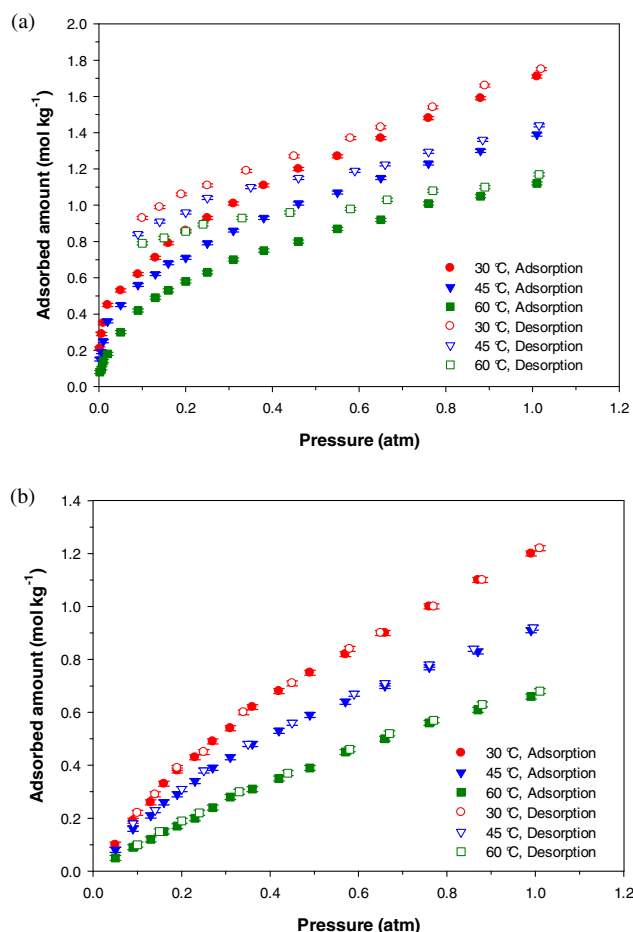


Fig. 2 – (a and b) Experimental adsorption–desorption isotherms of CO_2 on (a) modified and (b) untreated activated carbon measured at 30, 45 and 60°C . The error bars represent the standard deviation based on triplicate analysis. For points where the error bars are not visible, the error bars are smaller than the symbols used.

partial pressure increases, the slopes of the OXA-GAC adsorption isotherms decrease steeply compared with the slopes of the GAC adsorption isotherms, possibly in response to a decrease of CO_2 –nitrogen surface-group interactions. At low CO_2 partial pressures, the contribution of chemisorption to the total CO_2 uptake is more pronounced, whereas physisorption within the pores becomes significant at higher concentrations (Serna-Guerrero et al., 2010b). Nevertheless, the general trend for both adsorption isotherms was a steady increase in CO_2 uptake with increasing CO_2 pressure. As evident in the figures, the CO_2 adsorption was strongly dependent on the nitrogen functionalities: OXA-GAC exhibited a higher uptake than GAC over the whole pressure range studied. Notably, the reported values for the amount of carbon dioxide adsorbed were also in good agreement with the data from the cited literature for various ammonia-modified activated carbons (Pevida et al., 2008b; Plaza et al., 2009, 2011; Przepiórski et al., 2004).

Moreover, as shown in Fig. 2a and b, both of the adsorbents adsorbed less CO_2 at 45 and 60°C than at 30°C . The observed decrease in CO_2 uptakes at higher temperatures is attributed to the exothermic nature of the adsorption process, where both the molecular diffusion rate and the surface adsorption energy increase with increasing temperature (Maroto-Valer et al., 2005; Shafeeyan et al., 2011). According to the isothermal data, at 30°C and atmospheric feed pressure, the amount of CO_2 adsorbed by OXA-GAC was approximately 1.71 mol kg^{-1} ,

whereas only approximately 1.12 mol of CO₂/kg of the adsorbent was adsorbed at 60 °C. However, interestingly, the results at 45 °C and especially at 60 °C indicate that, compared to the unmodified adsorbent, OXA-GAC exhibited a smaller decrease in the amount adsorbed with increasing temperature. The modified adsorbent did exhibit a decrease in the amount adsorbed with increasing temperature; however, this decrease was not as pronounced as the uptake reduction observed for GAC, where physisorption is the only retention phenomenon. Because in the high-temperature adsorption, the contribution of chemisorption to the total adsorption is more significant; a possible explanation for this observation is the occurrence of strong chemical reactions between CO₂ and incorporated nitrogen-functionalities on the surface. These observations are consistent with the studies performed by Do and Wang (1998) and Na et al. (2001), who reported a decrease in the amount of CO₂ adsorbed onto commercial and Ajax-activated carbon from 3.2 to 1.6 mmol g⁻¹ and from 0.75 to 0.11 mmol g⁻¹ when the temperature was increased from 288 to 328 K and from 298 to 373 K, respectively, at 1 atm.

Furthermore, the reversibility of the adsorption process for both studied adsorbents was checked by measuring desorption isotherms. The isotherms of unmodified adsorbent (Fig. 2b) demonstrated the reversibility of the process at the various tested temperatures, as shown by the overlapping of the adsorption and desorption branches of the isotherms. This behavior is a typical feature of physisorption processes, where due to the weak adsorbent–adsorbate interactions the adsorbed molecules can be recovered during the desorption step as previously observed in many classical adsorbents such as activated carbons (Drage et al., 2009), zeolites (Cavenati et al., 2004) and metal organic framework (Bao et al., 2011). In comparison with the unmodified adsorbent, the adsorption and desorption isotherms of CO₂ on OXA-GAC did not follow the same path, indicating that CO₂ chemisorption is not completely reversible. The partial irreversibility observed in the isotherms of the modified sample may partly be a consequence of an irreversible reaction between CO₂ and nitrogen functionalities present on the carbon surfaces after modification. The observed increase in the desorption branch of the isotherms can also be attributed to diffusion resistance of CO₂ caused by the pore blocking with nitrogen surface groups that hinders the achievement of a strict equilibrium in the adsorption branch (Calleja et al., 2011; Olea et al., 2013; Bezerra et al., 2014). The trend seen in the adsorption/desorption isotherms of the modified sample is consistent with previous observations where it was shown that the contribution of chemisorption to the total CO₂ uptake is more pronounced at low CO₂ partial pressures and/or high-temperature adsorption.

3.3. Equilibrium isotherms modeling

Isotherm data analysis is generally a prerequisite to establish an equation that accurately predicts adsorption and that can be used to designing an adsorption separation process (Ho, 2004). As previously suggested, the overall CO₂ adsorption on the ammonia-modified activated carbon could be the result of both physical adsorption within the pores and chemical adsorption onto the nitrogen surface groups (Shafeeyan et al., 2011, 2012). Distinguishing between these two mechanisms is useful in identifying the factors that may affect the rate of the adsorption process (Lu et al., 2008; Su et al., 2010). Therefore, in the analysis of the adsorption equilibrium in the present study,

we implemented an approach that takes into account the physical adsorption as well as the enhanced adsorption due to chemical interactions. A semi-empirical model that considers the simultaneous occurrence of two independent chemical and physical adsorption mechanisms for CO₂ adsorption can be expressed as the following equation:

$$q = q_{\text{chem}} + q_{\text{phys}} \quad (5)$$

where q is the overall adsorption of CO₂ on ammonia-modified activated carbon, q_{chem} represents the CO₂ uptake by nitrogen functionalities and q_{phys} denotes the physical adsorption onto the porous structure.

According to Serna-Guerrero et al. (2010b), the essential prerequisite for the applicability of such an approach (assuming no interaction between the species adsorbed on each of the two types of adsorption sites) is the large difference between the adsorption energy of each adsorption site which results in a preferential adsorption of CO₂ on one of them at low surface coverage. Given that our results (Sections 3.2 and 3.4) indicate (i) an increased adsorption capacity for the modified adsorbent particularly at low concentrations, and (ii) a higher heat of adsorption for chemisorption at low coverage and reaching that of physisorption on the untreated sample at higher loading, the application of the above method seems to be acceptable.

To differentiate the contribution of each independent mechanism to the total adsorption capacity of the modified adsorbent, a procedure was used to calculate q_{phys} on the basis of the CO₂ adsorption data for the untreated activated carbon adsorbent. Using the method proposed by Serna-Guerrero et al. (2010b), the amount of CO₂ physisorbed onto the modified adsorbent was related the CO₂ uptake by the untreated activated carbon under the same operating conditions according to the following equation:

$$\frac{q_{\text{phys@P/P}_0}}{S} = \frac{q_{\text{GAC@P/P}_0}}{S_{\text{GAC}}} \quad (6)$$

where q_{GAC} and S_{GAC} are the CO₂ uptake and surface area of the untreated adsorbent, respectively, and S is the surface area of the modified adsorbent.

Eq. (6) was derived under the assumption that physisorption does not depend strongly on the nature of the surface whether it is the untreated adsorbent or its modified counterpart. Due to the weak interactions involved in physisorption, this is a reasonable assumption (Serna-Guerrero et al., 2010b). Serna-Guerrero et al. (2010b) also provided further evidence of the applicability of the assumption used in the present study and extended it to other adsorption processes that combine the contribution of physisorption and chemisorption mechanisms.

Using the equilibrium adsorption data for GAC, the corresponding values of q_{phys} for OXA-GAC at different temperatures were determined taking into account the difference in surface areas, according to Eq. (6). The contribution from chemical adsorption (q_{chem}) to the total CO₂ uptake is then calculated by subtracting the amount of q_{phys} from the overall adsorption uptake (q), measured experimentally for the modified sample. The corresponding values of q_{phys} and q_{chem} for the OXA-GAC adsorbent at different temperatures are represented in Fig. 3. As evident in this figure, the amount of CO₂ chemisorbed by the nitrogen functional groups corresponds to a type I isotherm in the IUPAC classification

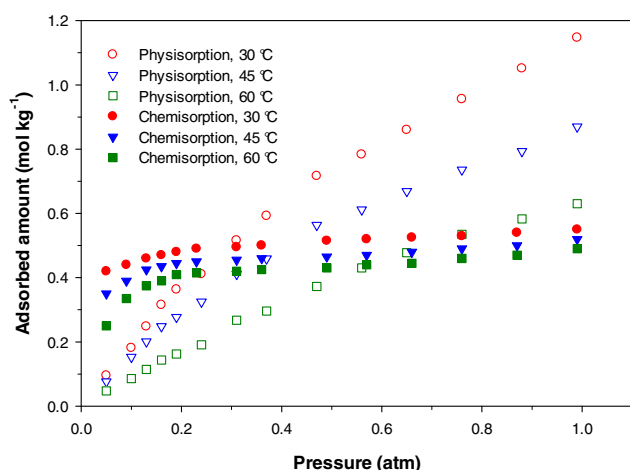


Fig. 3 – Calculated adsorption isotherms for CO₂ physisorption and chemisorption onto the modified adsorbent at 30, 45 and 60 °C.

scheme, consistent with adsorption due to chemical interactions.

After the contributions of the two independent physisorption and chemisorption mechanisms were distinguished, different equilibrium isotherm equations could potentially be used to correlate equilibrium data. Applying various conventional isotherm models, we can express the terms on the right side of Eq. (5) in different forms to describe each of the mechanisms with a proper isotherm model. The main distinguishing feature for selecting an appropriate isotherm model arises from the accuracy as well as simplicity of the equations. Non-idealities in the isotherms mainly stem from the heterogeneity of the adsorbent surface, and such heterogeneities often occur in the case of activated carbon (Malek and Farooq, 1996). From this point of view, three of the most common pure-species isotherm models (i.e., Freundlich, Sips and Toth) that have been previously applied to describe adsorption equilibria on heterogeneous adsorbents were employed in this work.

For each temperature and mechanism, a non-linear regression method was applied to independently determine the parameters corresponding to the aforementioned isotherm models. The optimal values of the Freundlich, Sips and Toth isotherm parameters are summarized in Tables 2–4, respectively. To quantitatively compare the quality of the nonlinear regressions for these three models, the average relative error (ARE) and nonlinear regression coefficient (R^2) were

Table 2 – Freundlich isotherm parameters with R^2 and ARE for each independent mechanism at temperatures of 303, 318, and 333 K.

| | Temperatures | | |
|--|--------------|-------|-------|
| | 303 K | 318 K | 333 K |
| Physical adsorption | | | |
| K_F (mol kg ⁻¹ atm ^{-1/m_F}) | 1.17 | 0.89 | 0.65 |
| m_F (dimensionless) | 1.22 | 1.38 | 1.43 |
| R^2 | 0.996 | 0.994 | 0.995 |
| ARE (%) | 5.54 | 5.99 | 5.72 |
| Chemical adsorption | | | |
| K_F (mol kg ⁻¹ atm ^{-1/m_F}) | 0.55 | 0.51 | 0.49 |
| m_F (dimensionless) | 11.67 | 9.60 | 6.53 |
| R^2 | 0.990 | 0.930 | 0.866 |
| ARE (%) | 0.69 | 1.82 | 5.18 |

Table 3 – Sips isotherm parameters with R^2 and ARE for each independent mechanism at temperatures of 303, 318, and 333 K.

| | Temperatures | | |
|-------------------------------|--------------|-------|-------|
| | 303 K | 318 K | 333 K |
| Physical adsorption | | | |
| q_m (mol kg ⁻¹) | 2.79 | 1.78 | 1.42 |
| K_S (atm ⁻¹) | 0.67 | 0.83 | 0.92 |
| m_S (dimensionless) | 1.07 | 1.04 | 0.98 |
| R^2 | 0.998 | 0.998 | 0.999 |
| ARE (%) | 2.52 | 2.27 | 1.83 |
| Chemical adsorption | | | |
| q_m (mol kg ⁻¹) | 0.69 | 0.55 | 0.48 |
| K_S (atm ⁻¹) | 10.29 | 23.06 | 57.58 |
| m_S (dimensionless) | 2.02 | 1.81 | 1.63 |
| R^2 | 0.983 | 0.955 | 0.963 |
| ARE (%) | 0.47 | 1.59 | 1.34 |

calculated; the results are included in Tables 2–4. As evident in these tables, the parameters of each isotherm model varied when the adsorption mechanism and temperature were changed. In the Freundlich model, the K_F parameter refers to the adsorption capacity and represents the adsorption quantity per unit equilibrium concentration, whereas the exponent $1/m_F$ is a measure of the adsorbent–adsorbate binding energy and expresses both the adsorption intensity and the surface heterogeneity (Ferraro et al., 2013). The higher values of K_F obtained for the physisorption mechanism indicated greater adsorption compared to chemisorption, whereas the higher values of m_F observed for chemisorption denoted a more favorable adsorption and a stronger bond between CO₂ and the modified adsorbent ($6 < m_F < 12$). The heterogeneity of the adsorbent surface can also be described with the exponent m_i in the Sips and Toth isotherm equations (Esteves et al., 2008). When the surface is homogeneous, m_i is equal to unity and the isotherm expressions reduce to the Langmuir equation. In agreement with the Freundlich model, the obtained values of the surface heterogeneity parameter in the Toth ($m_T < 1$) and Sips ($m_S > 1$) equations showed a higher degree of heterogeneous adsorption for CO₂ chemisorption. From Tables 3 and 4, the values of the saturation capacity parameter (q_m), which indicate the maximum amount that can possibly be adsorbed, decreased with increasing temperature.

Table 4 – Toth isotherm parameters with R^2 and ARE for each independent mechanism at temperatures of 303, 318, and 333 K.

| | Temperatures | | |
|-------------------------------|--------------------|--------------------|--------------------|
| | 303 K | 318 K | 333 K |
| Physical adsorption | | | |
| q_m (mol kg ⁻¹) | 3.57 | 1.96 | 1.01 |
| K_T (atm ⁻¹) | 0.66 | 0.99 | 1.41 |
| m_T (dimensionless) | 0.65 | 0.69 | 0.75 |
| R^2 | 0.999 | 0.999 | 0.999 |
| ARE (%) | 2.31 | 2.03 | 1.67 |
| Chemical adsorption | | | |
| q_m (mol kg ⁻¹) | 0.69 | 0.61 | 0.53 |
| K_T (atm ⁻¹) | 8.14×10^4 | 3.05×10^5 | 1.12×10^6 |
| m_T (dimensionless) | 0.27 | 0.28 | 0.29 |
| R^2 | 0.986 | 0.973 | 0.991 |
| ARE (%) | 0.41 | 0.94 | 0.33 |

Table 5 – Optimal values of the proposed Toth temperature-dependent parameters.

| | α (dimensionless) | η (dimensionless) | $(-\Delta H)$ (kJ mol ⁻¹) |
|---------------------|--------------------------|------------------------|---------------------------------------|
| Physical adsorption | 1.05 | 12.45 | 22.23 |
| Chemical adsorption | 0.22 | 2.62 | 73.24 |

The observed decrease is associated with the exothermicity of the adsorption process (Ning et al., 2012).

On the basis of the calculated values of ARE and R^2 tabulated in Tables 2–4, both the Sips and Toth isotherms were capable of fitting the equilibrium data over a broad range of experimental conditions. However, the Toth equation, which involves a symmetrical quasi-Gaussian distribution of adsorption sites, provided a slightly better fit. The low values obtained for the ARE (in no case greater than 3%), as well as the high values of the nonlinear regression coefficient (very near unity, $R^2 \geq 0.97$), indicate the goodness of the fit. Therefore, compared to the Freundlich and Sips models, the Toth equation is more accurate and more capable of describing the CO₂ adsorption isotherms over the ammonia-modified adsorbent. Thus, only the Toth model was used here to illustrate the quality of its fit to the experimental equilibrium data (Fig. 4). The complete form of the proposed semi-empirical model is expressed as follows:

$$q = \left[\frac{q_m K_T P}{(1 + (K_T P)^{m_T})^{1/m_T}} \right]_{\text{phys}} + \left[\frac{q_m K_T P}{(1 + (K_T P)^{m_T})^{1/m_T}} \right]_{\text{chem}} \quad (7)$$

where the subscripts “phys” and “chem” indicate the contributions of each independent mechanism to the total CO₂ uptake.

To express the temperature dependence of the Toth isotherm parameters for the purpose of interpolating or extrapolating the equilibrium data to various temperatures, as well as determining the isosteric enthalpy of adsorption,

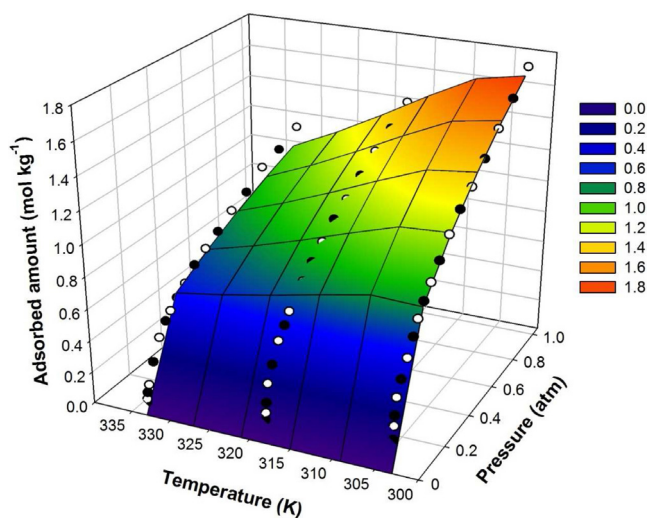


Fig. 4 – Graphical evaluation of the fit of the experimental equilibrium data to the proposed model for the modified adsorbent, whose parameters are presented in Tables 4 and 5. The surface is the global isotherm model, and the black and white circles show the experimental data at 303, 318 and 333 K.

the parameters, K_i , q_m and m_i are described by the following equations (Li and Tezel, 2008):

$$K_T = K_{T_0} \exp \left[-\frac{\Delta H}{RT_0} \left(\frac{T_0 - T}{T} \right) \right] \quad (8)$$

$$q_m = q_{m_0} \exp \left[\eta \left(\frac{T_0 - T}{T_0} \right) \right] \quad (9)$$

$$m_T = m_{T_0} + \alpha \left(\frac{T - T_0}{T} \right) \quad (10)$$

where T is the absolute temperature (K), T_0 is the reference temperature and was taken as 303 K, K_{i_0} and m_{i_0} are the affinity and heterogeneity parameters at the reference temperature, respectively, α and η are constant parameters, $(-\Delta H)$ is the isosteric heat of adsorption at zero coverage (kJ mol⁻¹), and R is the gas-law constant (J mol⁻¹ K⁻¹).

The optimal parameter values for both the chemical and physical adsorption mechanisms were obtained by nonlinear regression; the results are presented in Table 5. The surface obtained from the global fitting of the aforementioned model to the experimental data (Fig. 4) shows that the equilibrium data are described well for all temperatures when the adsorption isotherm plotted according to the proposed Toth equation is used.

Because η is the parameter that reflects the temperature dependence of q_m in the Toth isotherm (Eq. (9)), the lower values of η obtained for the chemisorption compared to the physisorption (Table 5) imply that, within the temperature range studied, the chemical adsorption mechanism exhibited a greater tendency to remain the same with changes in temperature. Furthermore, compared with physical adsorption, the chemisorption mechanism presented larger values of K_i (for instance, q_{chem} (8.14×10^4 atm⁻¹) compared to q_{phys} (6.6×10^{-1} atm⁻¹) at 303 K), which is attributed to the strength of the adsorbate–adsorbent interactions for the chemisorption mechanism (Do, 1998).

3.4. Isosteric heat of adsorption

The isosteric heat of adsorption is a critical parameter for designing and operating an adsorption-based separation process such as PSA. It is a measure of the interaction between the adsorbate molecules and the surface of the adsorbent, and it can be obtained from the temperature dependence of the adsorption isotherm (Esteves et al., 2008; Ning et al., 2012). The isosteric heat of adsorption, Q_{st} , also denoted as $-\Delta H$ (kJ mol⁻¹), at a specific adsorbate loading can be estimated using the Clausius–Clapeyron equation as follows (Park et al., 2002):

$$-\frac{Q_{\text{st}}}{R} = \left(\frac{\partial \ln P}{\partial 1/T} \right)_{q^a} \quad (11)$$

where q^a is a specific surface loading (mol kg⁻¹).

Integration of Eq. (11) enables the calculation of Q_{st} by knowing the differential partial pressure change as a

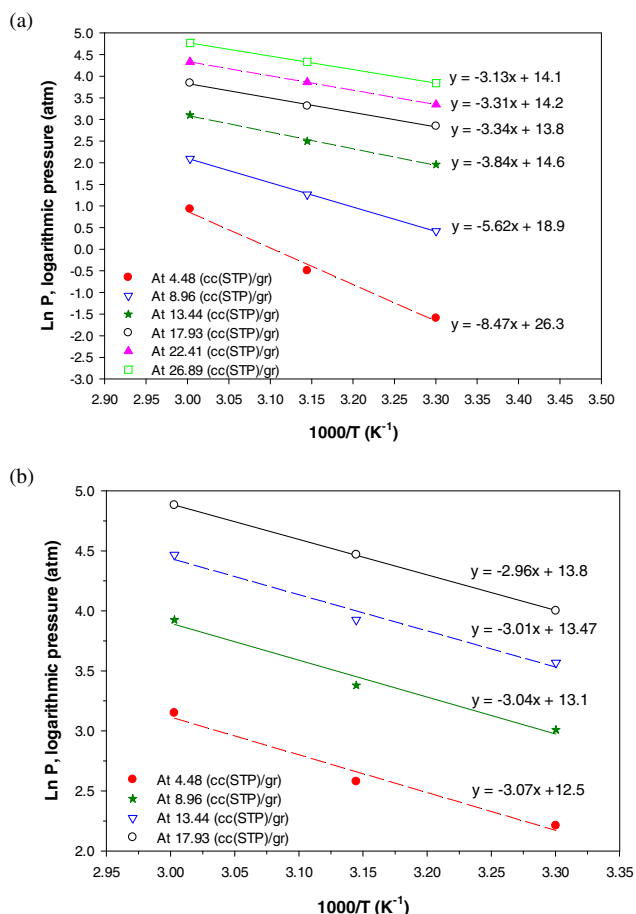


Fig. 5 – (a and b) Adsorption isotherms of CO₂ for (a) modified and (b) untreated adsorbent in the temperature range from 303 to 333 K. The points were calculated by numerical interpolation, and the lines represent the linear fit. All of the isotherms are marked with the corresponding amount of CO₂ adsorbed in units of (cm³ STP/g).

function of a differential change in system temperature for a given adsorbed amount:

$$Q_{st} = R \left[\frac{\ln P_1 - \ln P_2}{1/T_2 - 1/T_1} \right]_{q^a} \quad (12)$$

Therefore, the isosteric heats are obtained from the slopes of the lines in the plots of $\ln P$ vs. $1/T$ for the same adsorption amount for the different isotherms. In the present study, the experimental isotherms at the three temperatures of 303, 318, and 333 K for a given adsorption amount (from 0.2 to 1.2 mol kg⁻¹ in 0.2 mol kg⁻¹ increments) were used to measure the isosteric enthalpies of adsorption for OXA-GAC and GAC adsorbents (see Fig. 5a and b). The observed linear behavior is based on the assumption that, over the temperature range investigated, the isosteric heat of adsorption is independent of temperature and depends only on the surface coverage. In practice, the assumption of temperature independence of the heat of adsorption was shown to be valid for the pressure and loading estimations (Berlier and Frère, 1996; Esteves et al., 2008). Notably, consistent with the exothermic character of the adsorption process, negative Q_{st} values were attained at 303–333 K, indicating that the entropy was reduced in the system.

The isosteric enthalpy changes accompanying adsorption can be used to examine the molecular-scale interactions between the adsorbate molecules and the adsorbent.

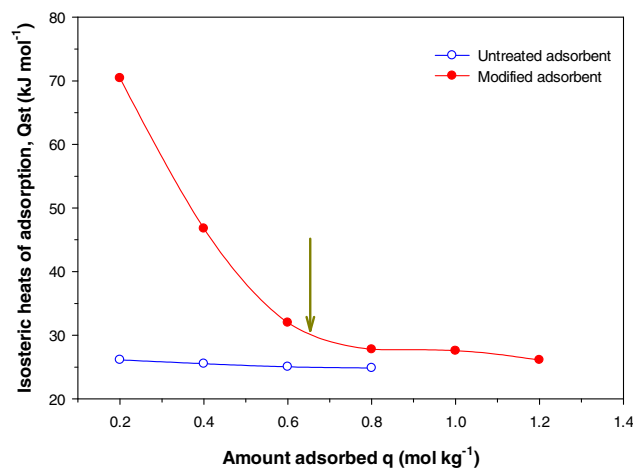


Fig. 6 – Concentration dependence of the isosteric enthalpy for CO₂ adsorption on the GAC and the OXA-GAC.

Moreover, information regarding the magnitude of the adsorption enthalpy and its surface coverage dependence can be used as criteria for determining the energetic heterogeneity of a solid surface (Belmabkhout and Sayari, 2009; Park et al., 2002). The isosteric heat is independent of the surface coverage when no interaction occurs between adsorbed molecules, and the surface is energetically homogeneous. However, a variation of the isosteric heats with the surface loading indicates the existence of different levels of surface energy and heterogeneity of the adsorbent surface (Ning et al., 2012). Fig. 6 depicts the variation of Q_{st} (calculated using the Clausius–Clapeyron equation) as a function of the amount of CO₂ adsorbed for the OXA-GAC and GAC adsorbents. As evident in the figure, the unmodified adsorbent exhibited approximately constant values of Q_{st} for different CO₂ loadings, indicating the uniform nature of the adsorbent surface. Notably, the obtained initial heat of adsorption for GAC (25.5 kJ mol⁻¹) corresponds closely to the value of $-\Delta H$ (22.2 kJ mol⁻¹) calculated from the temperature-dependent parameters of the proposed model for q_{phys} and is also of the same order of magnitude as the typical values for commercial activated carbon reported in the literature (Chue et al., 1995; Esteves et al., 2008; Garcés et al., 2013; Himeno et al., 2005; Van Der Vaart et al., 2000). In contrast, OXA-GAC exhibited rather high values of Q_{st} at the low range of loading, which reflects the relatively strong chemical interactions between CO₂ and the basic nitrogen functionalities.

The isosteric enthalpy of adsorption over OXA-GAC decreases with increasing CO₂ surface loading until it approaches values similar to those of the untreated carbon adsorbent. The observed decrease with increasing loading is attributed to the high degree of heterogeneity of the adsorbent surface (Belmabkhout and Sayari, 2009). At the beginning of the adsorption process, only the most active adsorption sites are filled, the activation energy is low and the heat of adsorption is high. With increasing surface coverage, less-active adsorption sites start to be occupied, thereby increasing the activation energy and decreasing the heat of adsorption (Himeno et al., 2007; Ning et al., 2012; Zhao et al., 2009). The observed heats of adsorption for the ammonia-modified adsorbent clearly demonstrate the strong and weak interactions of the nitrogen surface groups with CO₂ at low and high coverages, respectively. Notably, the Q_{st} value obtained at low coverage (70.5 kJ mol⁻¹) is consistent with the value calculated from the proposed Toth parameter K_i for q_{chem} (73.2 kJ mol⁻¹)

at zero loading and is in the range of values for typical cases of CO₂ chemisorption (60 to 90 kJ mol⁻¹) (Samanta et al., 2011). Indeed, this value is higher than that for a physical interaction but lower than that for a strong chemical interaction. In addition, in agreement with the observed inflection in the isotherms for CO₂ adsorption over the OXA-GAC adsorbent (see Fig. 2a), a corresponding curvature in the plot of the isosteric heat vs. coverage was detected, coinciding with the saturation of the most active adsorption sites (indicated by an arrow in Fig. 6). The observed variation of the slope of the Q_{st} vs. CO₂ loading curve clearly reflects the occurrence of two independent adsorption mechanisms.

4. Conclusions

The adsorption equilibria of carbon dioxide on an untreated GAC and its ammonia-modified counterpart were investigated over the temperature and pressure range of 303 to 333 K and up to pressures of 1 atm. Compared to untreated carbon, the OXA-GAC adsorbent exhibited a higher CO₂ uptake, particularly at low partial pressures. To distinguish the contribution of chemisorption and physisorption mechanisms to the overall CO₂ adsorption, we developed a semi-empirical equilibrium model. A non-linear regression method was employed to estimate the best fitting parameters corresponding to the isotherm model. An analysis of the calculated statistical parameters indicated that the proposed model successfully fit the experimental data over the entire analyzed ranges of temperature and pressure. The initial isosteric enthalpy of adsorption calculated using the Clausius–Clapeyron equation indicated a sharp increase in CO₂–adsorbent interaction after ammonia modification of the untreated adsorbent, consistent with a dramatic uptake of CO₂ at low partial pressures. The heats of adsorption calculated using the temperature-dependent parameters of the proposed model for physisorption and chemisorption of CO₂ onto the modified adsorbent were in excellent agreement with the heats of adsorption obtained from the experimental data. The findings of the present study are intended to be applied in future studies for developing and verifying a mathematical model capable of simulating the dynamic behavior of the fixed-bed adsorption of carbon dioxide.

Acknowledgements

The authors gratefully acknowledge High Impact Research (HIR) Grant from the University of Malaya for fully funding this study through the project number D000011-16001 and Bright Sparks Program. We also would like to thank the help from the instrument laboratory of Chemical Engineering Department, University of Malaya for providing the facility of BET analysis which supported by PG144-2012B.

References

- An, H., Feng, B., Su, S., 2009. CO₂ capture capacities of activated carbon fibre-phenolic resin composites. *Carbon* 47, 2396–2405.
- Arenillas, A., Smith, K.M., Drage, T.C., Snape, C.E., 2005. CO₂ capture using some fly ash-derived carbon materials. *Fuel* 84, 2204–2210.
- Bao, Z., Yu, L., Ren, Q., Lu, X., Deng, S., 2011. Adsorption of CO₂ and CH₄ on a magnesium-based metal organic framework. *J. Colloid Interface Sci.* 353, 549–556.
- Belmabkhout, Y., Sayari, A., 2009. Effect of pore expansion and amine functionalization of mesoporous silica on CO₂ adsorption over a wide range of conditions. *Adsorption* 15, 318–328.
- Berlier, K., Frère, M., 1996. Adsorption of CO₂ on activated carbon: simultaneous determination of integral heat and isotherm of adsorption. *J. Chem. Eng. Data* 41, 1144–1148.
- Bezerra, D., Oliveira, R., Vieira, R., Cavalcante Jr., C., Azevedo, D.S., 2011. Adsorption of CO₂ on nitrogen-enriched activated carbon and zeolite 13X. *Adsorption* 17, 235–246.
- Bezerra, D.P., Silva, F.W.M., Moura, P.A.S.d., Sousa, A.G.S.d., Vieira, R.S., Rodriguez-Castellon, E., Azevedo, D.C.S., 2014. CO₂ adsorption in amine-grafted zeolite 13X. *Appl. Surf. Sci.* 314, 314–321.
- Cavenati, S., Grande, C.A., Rodrigues, A.E., 2004. Adsorption equilibrium of methane, carbon dioxide, and nitrogen on zeolite 13X at high pressures. *J. Chem. Eng. Data* 49, 1095–1101.
- Calleja, G., Sanz, R., Arencibia, A., Sanz-Pérez, E.S., 2011. Influence of drying conditions on amine-functionalized SBA-15 as adsorbent of CO₂. *Top. Catal.* 54, 135–145.
- Chue, K.T., Kim, J.N., Yoo, Y.J., Cho, S.H., Yang, R.T., 1995. Comparison of activated carbon and zeolite 13X for CO₂ recovery from flue gas by pressure swing adsorption. *Ind. Eng. Chem. Res.* 34, 591–598.
- Delgado, J.A., Uguina, M.A., Sotelo, J.L., Ruiz, B., Gomez, J.M., 2006. Fixed-bed adsorption of carbon dioxide/methane mixtures on silicalite pellets. *Adsorption* 12, 5–18.
- Do, D.D., 1998. *Adsorption Analysis: Equilibria and Kinetics*. World Scientific, Singapore.
- Do, D.D., Wang, K., 1998. A new model for the description of adsorption kinetics in heterogeneous activated carbon. *Carbon* 36, 1539–1554.
- Drage, T.C., Arenillas, A., Smith, K.M., Pevida, C., Piippo, S., Snape, C.E., 2007. Preparation of carbon dioxide adsorbents from the chemical activation of urea-formaldehyde and melamine-formaldehyde resins. *Fuel* 86, 22–31.
- Drage, T.C., Blackman, J.M., Pevida, C., Snape, C.E., 2009. Evaluation of activated carbon adsorbents for CO₂ capture in gasification. *Energy Fuels* 23, 2790–2796.
- Esteves, I.A.A.C., Lopes, M.S.S., Nunes, P.M.C., Mota, J.P.B., 2008. Adsorption of natural gas and biogas components on activated carbon. *Sep. Purif. Technol.* 62, 281–296.
- Ferraro, V., Cruz, I.B., Jorge, R.F., Pintado, M.E., Castro, P.M.L., 2013. Effects of physical parameters onto adsorption of the borderline amino acids glycine, lysine, taurine, and tryptophan upon amberlite XAD16 resin. *J. Chem. Eng. Data* 58, 707–717.
- Foo, K.Y., Hameed, B.H., 2010. Insights into the modeling of adsorption isotherm systems. *Chem. Eng. J.* 156, 2–10.
- Garcés, S.I., Villarroel-Rocha, J., Sapag, K., Korili, S.A., Gil, A., 2013. Comparative study of the adsorption equilibrium of CO₂ on microporous commercial materials at low pressures. *Ind. Eng. Chem. Res.* 52, 6785–6793.
- Gomes, V.G., Yee, K.W.K., 2002. Pressure swing adsorption for carbon dioxide sequestration from exhaust gases. *Sep. Purif. Technol.* 28, 161–171.
- Grande, C.A., Rodrigues, A.E., 2004. Adsorption kinetics of propane and propylene in zeolite 4A. *Chem. Eng. Res. Des.* 82, 1604–1612.
- Himeno, S., Komatsu, T., Fujita, S., 2005. High-pressure adsorption equilibria of methane and carbon dioxide on several activated carbons. *J. Chem. Eng. Data* 50, 369–376.
- Himeno, S., Tomita, T., Suzuki, K., Yoshida, S., 2007. Characterization and selectivity for methane and carbon dioxide adsorption on the all-silica DD3R zeolite. *Microporous Mesoporous Mater.* 98, 62–69.
- Ho, Y.-S., 2004. Selection of optimum sorption isotherm. *Carbon* 42, 2115–2116.
- Ho, Y.S., Porter, J.F., McKay, G., 2002. Equilibrium isotherm studies for the sorption of divalent metal ions onto peat: Copper, nickel and lead single component systems. *Water Air Soil Pollut.* 141, 1–33.

- Houshmand, A., Daud, W.M.A.W., Shafeeyan, M.S., 2011a. Tailoring the surface chemistry of activated carbon by nitric acid: study using response surface method. *Bull. Chem. Soc. Jpn.* 84, 1251–1260.
- Houshmand, A., Wan Daud, W.M.A., Shafeeyan, M.S., 2011b. Exploring potential methods for anchoring amine groups on the surface of activated carbon for CO₂ adsorption. *Sep. Sci. Technol.* 46, 1098–1112.
- Houshmand, A., Daud, W.M.A.W., Lee, M.G., Shafeeyan, M.S., 2012. Carbon dioxide capture with amine-grafted activated carbon. *Water, Air, Soil Pollut.* 223, 827–835.
- Houshmand, A., Shafeeyan, M.S., Arami-Niya, A., Daud, W.M.A.W., 2013. Anchoring a halogenated amine on the surface of a microporous activated carbon for carbon dioxide capture. *J. Taiwan Inst. Chem. Eng.* 44, 774–779.
- Jadhav, P.D., Chatti, R.V., Biniwale, R.B., Labhsetwar, N.K., Devotta, S., Rayalu, S.S., 2007. Monoethanol amine modified zeolite 13x for CO₂ adsorption at different temperatures. *Energy Fuels* 21, 3555–3559.
- Knowles, G.P., Delaney, S.W., Chaffee, A.L., 2006. Diethylenetriamine[propyl(silyl)]-functionalized (DT) mesoporous silicas as CO₂ adsorbents. *Ind. Eng. Chem. Res.* 45, 2626–2633.
- LeVan, M.D., Carta, G., Yon, C.M., 1999. Adsorption and ion exchange. In: Green, D.W. (Ed.), *Perry's Chemical Engineers' Handbook*, 7th ed. McGrawHill, New York, NY.
- Li, P., Tezel, F.H., 2008. Pure and binary adsorption equilibria of carbon dioxide and nitrogen on silicalite. *J. Chem. Eng. Data* 53, 2479–2487.
- Lu, C., Bai, H., Wu, B., Su, F., Hwang, J.F., 2008. Comparative study of CO₂ capture by carbon nanotubes, activated carbons, and zeolites. *Energy Fuels* 22, 3050–3056.
- Lu, C., Su, F., Hsu, S.-C., Chen, W., Bai, H., Hwang, J.F., Lee, H.-H., 2009. Thermodynamics and regeneration of CO₂ adsorption on mesoporous spherical-silica particles. *Fuel Process. Technol.* 90, 1543–1549.
- Malek, A., Farooq, S., 1996. Comparison of isotherm models for hydrocarbon adsorption on activated carbon. *AIChE J.* 42, 3191–3201.
- Maroto-Valer, M.M., Tang, Z., Zhang, Y., 2005. CO₂ capture by activated and impregnated anthracites. *Fuel Process. Technol.* 86, 1487–1502.
- Mason, J.A., Sumida, K., Herm, Z.R., Krishna, R., Long, J.R., 2011. Evaluating metal-organic frameworks for post-combustion carbon dioxide capture via temperature swing adsorption. *Energy Environ. Sci.* 4, 3030–3040.
- Mulgundmath, V., Tezel, F.H., 2010. Optimisation of carbon dioxide recovery from flue gas in a TPSA system. *Adsorption* 16, 587–598.
- Mutasim, Z.Z., Bowen, J.H., 1991. Pressure swing adsorption in non-isothermal, non-equilibrium conditions: single adsorbate. *Chem. Eng. Res. Des.* 69, 108–118.
- Na, B.-K., Koo, K.-K., Eum, H.-M., Lee, H., Song, H., 2001. CO₂ recovery from flue gas by PSA process using activated carbon. *Korean J. Chem. Eng.* 18, 220–227.
- Ning, P., Li, F., Yi, H., Tang, X., Peng, J., Li, Y., He, D., Deng, H., 2012. Adsorption equilibrium of methane and carbon dioxide on microwave-activated carbon. *Sep. Purif. Technol.* 98, 321–326.
- Olea, A., Sanz-Pérez, E.S., Arencibia, A., Sanz, R., Calleja, G., 2013. Amino-functionalized pore-expanded SBA-15 for CO₂ adsorption. *Adsorption* 19, 589–600.
- Park, J.-W., Lee, S.-S., Choi, D.-K., Lee, Y.-W., Kim, Y.-M., 2002. Adsorption equilibria of toluene, dichloromethane, and trichloroethylene onto activated carbon fiber. *J. Chem. Eng. Data* 47, 980–983.
- Pereira, M.F.R., Soares, S.F., Órfão, J.J., Figueiredo, J.L., 2003. Adsorption of dyes on activated carbons: influence of surface chemical groups. *Carbon* 41, 811–821.
- Pevida, C., Drage, T.C., Snape, C.E., 2008a. Silica-templated melamine-formaldehyde resin derived adsorbents for CO₂ capture. *Carbon* 46, 1464–1474.
- Pevida, C., Plaza, M.G., Arias, B., Feroso, J., Rubiera, F., Pis, J.J., 2008b. Surface modification of activated carbons for CO₂ capture. *Appl. Surf. Sci.* 254, 7165–7172.
- Plaza, M.G., Garcia, S., Rubiera, F., Pis, J.J., Pevida, C., 2011. Evaluation of ammonia modified and conventionally activated biomass based carbons as CO₂ adsorbents in postcombustion conditions. *Sep. Purif. Technol.* 80, 96–104.
- Plaza, M.G., Pevida, C., Arenillas, A., Rubiera, F., Pis, J.J., 2007. CO₂ capture by adsorption with nitrogen enriched carbons. *Fuel* 86, 2204–2212.
- Plaza, M.G., Pevida, C., Arias, B., Feroso, J., Casal, M.D., Martín, C.F., Rubiera, F., Pis, J.J., 2009. Development of low-cost biomass-based adsorbents for postcombustion CO₂ capture. *Fuel* 88, 2442–2447.
- Plaza, M.G., Rubiera, F., Pis, J.J., Pevida, C., 2010. Ammoxidation of carbon materials for CO₂ capture. *Appl. Surf. Sci.* 256, 6843–6849.
- Porter, J.F., McKay, G., Choy, K.H., 1999. The prediction of sorption from a binary mixture of acidic dyes using single- and mixed-isotherm variants of the ideal adsorbed solute theory. *Chem. Eng. Sci.* 54, 5863–5885.
- Przepiórski, J., Skrodziewicz, M., Morawski, A.W., 2004. High temperature ammonia treatment of activated carbon for enhancement of CO₂ adsorption. *Appl. Surf. Sci.* 225, 235–242.
- Rinker, E.B., Ashour, S.S., Sandall, O.C., 2000. Absorption of carbon dioxide into aqueous blends of diethanolamine and methyldiethanolamine. *Ind. Eng. Chem. Res.* 39, 4346–4356.
- Rodríguez-Reinoso, F., Lahaye, J., Ehrburger, P., 1991. *Fundamental Issues in Control of Carbon Gasification Reactivity*. Kluwer Academic, Dordrecht.
- Rouquerol, F., Rouquerol, J., Sing, K., 1999. *Adsorption by Powders & Porous Solids: Principles, Methodology and Applications*. Academic, London.
- Samanta, A., Zhao, A., Shimizu, G.K.H., Sarkar, P., Gupta, R., 2011. Post-combustion CO₂ capture using solid sorbents: a review. *Ind. Eng. Chem. Res.* 51, 1438–1463.
- Serna-Guerrero, R., Belmabkhout, Y., Sayari, A., 2010a. Further investigations of CO₂ capture using triamine-grafted pore-expanded mesoporous silica. *Chem. Eng. J.* 158, 513–519.
- Serna-Guerrero, R., Belmabkhout, Y., Sayari, A., 2010b. Modeling CO₂ adsorption on amine-functionalized mesoporous silica: 1. A semi-empirical equilibrium model. *Chem. Eng. J.* 161, 173–181.
- Shafeeyan, M.S., Daud, W.M.A.W., Houshmand, A., Arami-Niya, A., 2011. Ammonia modification of activated carbon to enhance carbon dioxide adsorption: effect of pre-oxidation. *Appl. Surf. Sci.* 257, 3936–3942.
- Shafeeyan, M.S., Daud, W.M.A.W., Houshmand, A., Shamiri, A., 2010. A review on surface modification of activated carbon for carbon dioxide adsorption. *J. Anal. Appl. Pyrolysis* 89, 143–151.
- Shafeeyan, M.S., Wan Daud, W.M.A., Houshmand, A., Arami-Niya, A., 2012. The application of response surface methodology to optimize the amination of activated carbon for the preparation of carbon dioxide adsorbents. *Fuel* 94, 465–472.
- Shafeeyan, M.S., Wan Daud, W.M.A., Shamiri, A., 2014. A review of mathematical modeling of fixed-bed columns for carbon dioxide adsorption. *Chem. Eng. Res. Des.* 92, 961–988.
- Shafeeyan, M.S., Houshmand, A., Arami-Niya, A., Razaghizadeh, H., Daud, W.M.A.W., 2015. Modification of activated carbon using nitration followed by reduction for carbon dioxide capture. *Bull. Korean Chem. Soc.* 36, 533–538.
- Sing, K.S.W., 1998. Adsorption methods for the characterization of porous materials. *J. Colloid Interface Sci.* 76–77, 3–11.
- Siriwardane, R.V., Shen, M.-S., Fisher, E.P., Poston, J.A., 2001. Adsorption of CO₂ on molecular sieves and activated carbon. *Energy Fuels* 15, 279–284.
- Sjostrom, S., Krutka, H., 2010. Evaluation of solid sorbents as a retrofit technology for CO₂ capture. *Fuel* 89, 1298–1306.

- Su, F., Lu, C., Kuo, S.-C., Zeng, W., 2010. Adsorption of CO₂ on amine-functionalized Y-type zeolites. *Energy Fuels* 24, 1441–1448.
- Van Der Vaart, R., Huiskes, C., Bosch, H., Reith, T., 2000. Single and mixed gas adsorption equilibria of carbon dioxide/methane on activated carbon. *Adsorption* 6, 311–323.
- Veawab, A., Tontiwachwuthikul, P., Chakma, A., 1999. Corrosion behavior of carbon steel in the CO₂ absorption process using aqueous amine solutions. *Ind. Eng. Chem. Res.* 38, 3917–3924.
- Xu, X., Song, C., Andresen, J.M., Miller, B.G., Scaroni, A.W., 2002. Novel polyethylenimine-modified mesoporous molecular sieve of MCM-41 type as high-capacity adsorbent for CO₂ capture. *Energy Fuels* 16, 1463–1469.
- Yong, Z., Mata, V., Rodrigues, A.r.E., 2002. Adsorption of carbon dioxide at high temperature—a review. *Sep. Purif. Technol.* 26, 195–205.
- Zhang, Z., Xu, M., Wang, H., Li, Z., 2010. Enhancement of CO₂ adsorption on high surface area activated carbon modified by N₂, H₂ and ammonia. *Chem. Eng. J.* 160, 571–577.
- Zhao, X.-X., Xu, X.-L., Sun, L.-B., Zhang, L.L., Liu, X.-Q., 2009. Adsorption behavior of carbon dioxide and methane on AlPO₄-14: a neutral molecular sieve. *Energy Fuels* 23, 1534–1538.